Dalton Transactions

Accepted Manuscript

ROYAL SOCIETY OF CHEMISTRY

www.rsc.org/dalton

Salen–type Dy_4 single–molecule magnet with enhanced energy barrier and its analogues

Fang Luan,[a,b] Pengfei Yan,[a] Jing Zhu,[a] Tianqi Liu,[a] Xiaoyan Zou,[a] Guangming Li*[a]

[a] *Key Laboratory of Functional Inorganic Material Chemistry (MOE), School of Chemistry and Materials Science, Heilongjiang University, No. 74, Xuefu Road, Nangang District, Harbin, Heilongjiang 150080, P. R. China, E-mail: gmli_2000@163.com. Fax: (+86)451-86608458; Tel: (+86)451-86608458*

[b] *School of Pharmacy, Jiamusi University, Jiamusi, Heilongjiang 154007 (P. R. China)*

†Electronic supplementary information (ESI) available: Additional magnetic measurements, IR, UV–vis, Powder X–ray diffraction, TG–DSC, Selected bond lengths and angles for **1**–**4**, CIF document. CCDC No. 1000758−1000761 for **1**–**4**. For crystallographic data in CIF or other electronic format see DOI:

Four isomorphic tetranuclear lanthanide complexes, namely, $[Ln_4(L)_2(HL)_2(NO_3)_2(OH)_2](NO_3)_2{\cdot}4H_2O$ (Ln = Dy (**1**); Tb (**2**); Ho (**3**); Er (**4**)), constructed by hexadentate salen–type ligand *N,N'*-bis(3-methoxy-salicylidene)cyclohexane-1,2-diamine, have been isolated. X–ray crystallographic analysis reveals that all complexes **1**−**4** are of discrete tetranuclear structure with a unique $\{Ln_4O_8\}$ core in which four lanthanide ions are coplanar in a rhombic frame. Two crystallographically unequivalent lanthanide ions that $Ln1^{III}$ ion is nine–coordinated in monocapped square–antiprismatic geometry of C_{4v} point group and $Ln2^{III}$ ion is eight–coordinated in distorted bicapped trigonal–prismatic geometry of C_{2v} point group. Magnetic analysis reveals that complex **1** exhibits two slow magnetic relaxations with the highest energy barrier among the reported tetranuclear salen–type dysprosium SMMs. It further extends the SMMs of salen–type lanthanide complexes.

Introduction

Single–molecule magnets (SMMs) exhibiting slow magnetic relaxation below the blocking temperature have attracted considerable attention in chemistry, physics and materials science since 1990s.[1] It may be attributed to their unique and intriguing properties and potential applications in

high–density information storage,[2] quantum computing[3] and molecule–based spintronics devices[4]. SMMs can be verified on the basis of the three parameters: the magnetic blocking temperature (T_B), the strength of the coercive magnetic field (H_c) and the anisotropy barrier (U_{eff}), among which the parameter of U_{eff} is the most common one used for judging the quality of the SMMs.[5] In contrast to the transition metal SMMs,[6] special attention has been focused on the lanthanide SMMs since 2003[7] due to their strong angular dependence of 4f orbitals and high substantial anisotropy. The slow magnetic relaxation of lanthanide SMMs high likely results from their combined ligand field sublevel splitting generating the uniaxial magnetic anisotropy and (2J+1)–fold electronic levels, which gives large thermal energy barrier between the ground states and the second lowest sublevels. In the past decade, a number of lanthanide SMMs have been presented.[5, 8] Predominant amongst the factors distinguishing the f–elements as spin–carriers for single–molecule magnets is their unparalleled single–ion anisotropy. It is noteworthy that the Dy^{III} ion contributes much more than other lanthanide ions,[9] because Dy^{III} ion possessing $4f^9$ substantial anisotropy is a kind of Kramers' ion with bistable ground state. To date, the largest effective energy barrier of dysprosium–SMM was 528 K reported by Blagg R. J. et al. in 2011,[10] although the record of effective energy barrier in lanthanide SMMs field is still kept by [Tb^{III}(Pc)(Pc′)] (U_{eff} = 939K / 652cm^{-1}).[11] It is known that the ligand plays essential role on achieving lanthanide SMMs with defined geometries and particular magnetic properties.[12] The remarkable magnetic characteristics of the f−elements are contingent upon the interaction between the single−ion electron density and the crystal field environment. This interaction leads to the increased single−ion anisotropies requisite for strong single–molecule magnets. Therefore, constructing a coordination environment of the lanthanide ion judiciously can increase single−ion anisotropy simply.[13] Salen–type as a suitable ligand has been extensively employed in the synthesis of salen type lanthanide SMMs. Several salen type lanthanide complexes with single molecular magnetic behavior have been documented, e.g., salen–type dinuclear,[14] trinuclear,[15] tetranuclear[16] and 1D chain[14g] Dy–SMMs have been reported. In view of recent important progress in salen–type lanthanide SMMs as well as our longstanding research on the structure,[17] luminescence[18] and magnetic properties[19] of salen–type lanthanide complexes, the semi–rigid N,N′-bis(3-methoxy-salicylidene)cyclohexane-1,2-diamine (H_2L) has been employed to explore the effect of the ligand on the magnetism of the lanthanide ions. As a

result, a series of four salen–type tetranuclear lanthanide complexes have been synthesized and isolated. X−ray crystallographic analysis reveals that all complexes **1**−**4** are isomorphic featuring tetranuclear structure with a unique $\{Ln_4O_8\}$ core in which four lanthanide ions are coplanar in a rhombic frame. Magnetic studies indicate that complex **1** exhibits two slow magnetic relaxation processes with effective energy barrier of 48.14 K.

Experimental Section

Materials and Methods

All manipulations were performed under ambient conditions. All chemicals and solvents except $Ln(NO_3)_3{\cdot}6H_2O$ (Ln = Dy, Tb, Ho, Er) and H_2L were commercial products of reagent grade and were used without further purification. H_2L (*N*,*N'*-bis(3-methoxy-salicylidene)cyclohexane-1,2-diamine) was synthesized according to the reported method.[20] Elemental analyses (C, H and N) were performed on a Perkin–Elmer 2400 analyzer. UV spectra data were collected on a Perkin–Elmer 35 spectrophotometer. FT−IR spectra were collected on a Perkin–Elmer 100 spectrophotometer from 4000 to 500 cm^{-1} using powder sample in KBr pellets. Thermal analyses were carried out on a STA–6000 in the range of 30 °C to 800 °C with a heating rate of 10 °C min^{-1} under the N_2 atmosphere. Powder X–ray diffraction (PXRD) data were recorded on a Rigaku D / Max−3B X−ray diffractometer with Cu Kα as the radiation source (λ = 0.15406 nm) in the angular range θ = 5–50º at room temperature (the samples were grinded to be flat sample holders). The magnetic susceptibilities of complexes **1**−**4** (polycrystalline samples without being restrained by eicosane**)** were measured by Quantum Design SQUID MPMS–XL7 magnetometer.

X−ray Crystallographic Structures

Single crystals of complexes **1**−**4** were selected at 293 ± 2 K for X−ray diffraction analysis on an Oxford Xcalibur Gemini Ultra diffractometer using graphite−monochromated Mo–Kα radiation (λ = 0.71073 Å). The data sets were corrected by empirical absorption correction using spherical harmonics, implemented in SCALE3 ABSPACK scaling algorithm.[21] The structures were solved by direct

methods and all non–hydrogen atoms are refined anisotropically by full matrix least–squares on F^2 using the SHELXTL–97 program.[22] Selected crystallographic data and structure refinement parameters are given in Table 1. CCDC No. 1000758−1000761 for **1**−**4** contains the supplementary crystallographic data for this paper. The selected bond lengths and bond angles for complexes **1**−**4** are summarized in Table S1−4. These data can be obtained free of charge from the Cambridge Crystallographic Data Centre via www.ccdc.cam.ac.uk/data_request/cif.

Synthesis of $[Dy_4(L)_2(HL)_2(NO_3)_2(OH)_2](NO_3)_2\cdot 4H_2O$ (1)

H_2L (0.1 mmol, 38.3 mg) was dissolved in MeOH / DMF (9 mL, 2:1) in the presence of triethylamine (0.30 mmol, 42 μL), then $Dy(NO_3)_3\cdot 6H_2O$ (0.1 mmol, 45.7 mg) was added under stirring. The clear yellow solution was stirred for 10 minutes, and then filtered. The diethyl ether was allowed to diffuse slowly into the filtrate at ambient temperature. The suitable yellow block–shaped crystals were obtained after 6 days. Yield: 41mg (65%). Elemental analysis (%) calcd for $C_{88}H_{100}Dy_4N_{12}O_{33.96}$ (2519.17): C 41.96, H 4.00, N 6.67; found: C 41.94, H 4.02, N 6.67. IR (KBr, cm^{-1}): 3421, 2938, 2857, 1645, 1611, 1474, 1287, 1225, 1167, 1072, 786, 735.

Synthesis of $[Tb_4(L)_2(HL)_2(NO_3)_2(OH)_2](NO_3)_2\cdot 4H_2O$ (2)

The complex was synthesized with the same procedure to complex **1** except $Tb(NO_3)_3\cdot 6H_2O$ (0.1 mmol, 45.3 mg) was used instead of $Dy(NO_3)_3\cdot 6H_2O$. Yield: 31 mg (50%). Elemental analysis (%) calcd for $C_{88}H_{100}Tb_4N_{12}O_{33.96}$ (2504.89): C 42.20, H 4.02, N 6.71; found: C 42.12, H 4.05, N 6.74. IR (KBr, cm^{-1}): 3423, 2937, 2854, 1651, 1618, 1450, 1288, 1227, 1166, 1072, 785, 742.

Synthesis of $[Ho_4(L)_2(HL)_2(NO_3)_2(OH)_2](NO_3)_2\cdot 4H_2O$ (3)

The complex was synthesized with the same procedure to complex **1** except $Ho(NO_3)_3\cdot 6H_2O$ (0.1 mmol, 45.9 mg) was used instead of $Dy(NO_3)_3\cdot 6H_2O$. Yield: 37 mg (59%). Elemental analysis (%) calcd for $C_{88}H_{100}Ho_4N_{12}O_{33.96}$ (2528.89): C 41.79, H 3.99, N 6.65; found: C 41.81, H 4.02, N 6.64. IR (KBr, cm^{-1}): 3429, 2931, 2857, 1645, 1611, 1467, 1288, 1230, 1166, 1079, 782, 736.

Table 1 Crystal data and structure refinement for complexes **1-4**

Complexes	**1**	**2**	**3**	**4**
CCDC No.	1000758	1000759	1000760	1000761
Formula	$C_{88}H_{100}Dy_4N_{12}O_{33.96}$	$C_{88}H_{100}Tb_4N_{12}O_{33.96}$	$C_{88}H_{100}Ho_4N_{12}O_{33.96}$	$C_{88}H_{100}Er_4N_{12}O_{33.96}$
Formula weight	2519.17	2504.89	2537.58	2538.21
Crystal system	Triclinic	Triclinic	Triclinic	Triclinic
Space group	$P\bar{1}$	$P\bar{1}$	$P\bar{1}$	$P\bar{1}$
a (Å)	14.4293(7)	14.4379(7)	14.4145(6)	14.4223(9)
b (Å)	14.5421(9)	14.5620(5)	14.5348(8)	14.5202(9)
c (Å)	14.7018(8)	14.7018(7)	14.6776(8)	14.6662(8)
α (º)	111.061(5)	110.979(4)	111.197(5)	111.232(5)
β (º)	104.181(4)	104.156(4)	104.067(4)	104.018(5)
γ (º)	107.967(5)	107.975(4)	107.837(4)	107.831(5)
V (Å^3)	2508.8(2)	2516.30(19)	2503.0(2)	2500.2(3)
Z	1	1	1	1
D_{calcd} (mg cm^3)	1.667	1.653	1.683	1.692
μ (mm^{-1})	3.030	2.862	3.213	3.408
F (000)	1248	1244	1260	1264
θ range(º)	2.86-25.00	2.94-25.00	2.94-25.00	2.92-25.00
Reflection collected	19128	19577	19711	18793
Unique reflection	8819	8841	8793	8786
R_{int}	0.0339	0.0310	0.0383	0.0338
R_1, [$I > 2\sigma(I)$]	0.0351	0.0328	0.0370	0.0353
wR_2, [$I > 2\sigma(I)$]	0.0819	0.0820	0.0865	0.0829
R_1, (all data)	0.0516	0.0473	0.0546	0.0506
wR_2, (all data)	0.0930	0.0918	0.0995	0.0938
GOF on F^2	1.074	1.068	1.055	1.047

Synthesis of $[Er_4(L)_2(HL)_2(NO_3)_2(OH)_2](NO_3)_2\cdot 4H_2O$ (4)

The complex was synthesized with the same procedure to complex **1** except $Er(NO_3)_3\cdot 6H_2O$ (0.1 mmol, 46.1 mg) was used instead of $Dy(NO_3)_3\cdot 6H_2O$. Yield: 35 mg (55%). Elemental analysis (%) calcd for $C_{88}H_{100}Er_4N_{12}O_{33.96}$ (2538.21): C 41.64, H 3.97, N 6.62; found: C 41.66, H 4.01, N 6.59. IR (KBr, cm^{-1}): 3422, 2937, 2857, 1651, 1611, 1456, 1285, 1227, 1166, 1072, 789, 736.

Results and Discussion

Descriptions of the Structures

X–ray crystallographic analysis reveals that all complexes **1**–**4** are isomorphic discrete tetranuclear structures crystallizing in a triclinic space group of $P\bar{1}$. In a typical structure of complex **1** (Fig. 1), there are four Dy^{III} ions, four ligands, two μ_3–OH^-, and two nitrate anions. Four Dy^{III} ions form a unique $\{Ln_4O_8\}$ core in which the four lanthanide ions are coplanar in a rhombic frame. The distance of Dy1–Dy2 is 3.5043(4) Å and the distance of Dy1–Dy2a is 3.8524(5) Å. Two triply bridging hydroxide atoms (O12 and O12a) are located on the opposite of the Dy_4 plane and displaced out of that plane by 0.9349 Å. The two μ_3–O are apart from each other approximately 2.7354 Å, the angles of Dy–(μ_3–O)–Dy are 96.47(15)º, 110.44(14)º, 107.91(14)º and the Dy–(μ_3–O) distances are 2.369(4), 2.330(4), 2.321(4) Å, respectively. It differs from the reported $\{Ln_4O_6\}$[16b] cores in which every two adjacent Dy^{III} ions are bridged by a pair of phenoxide O atoms from different ligands producing a stretch rhombus structure. Simultaneously, complex **1** also differs from another reported $\{Ln_4O_7\}$[14h] cores in which the central μ_4-O atom links four Dy^{III} ions and two adjacent Dy^{III} ions are bridged by deprotonated phenol oxygen atoms from an L^{2-} ligand.

The crystallographically equivalent $Dy1^{III}$ and $Dy1a^{III}$ center ions lies in a monocapped squared antiprism nine–coordinated geometry with C_{4v} point group, (Fig. 1b) which is defined

by seven O–donors from two deprotoned salen–type ligands. The distances range of Dy1–O bonds is 2.266 to 2.695 Å. The crystallographic equivalent $Dy2^{III}$ and $Dy2a^{III}$ center ions lies in a distorted bicapped trigonal prism eight–coordinated geometry with C_{2v} point group, which is defined by four O–donors and two N–donors from two deprotoned salen–type ligands. The Dy2–O bond distances are in the range of 2.312 to 2.494 Å, and the distances of Dy2–N3 and Dy2–N4 are 2.419 Å and 2.505 Å, respectively. The selected bond distances (Å) and angles (º) are presented in Table S1–4. Notably, it differ from the reported salen–type complex of $[Dy_4(salen)_6]\cdot 5.5H_2O$ with the geometry of Dy1 is eight–coordinate sphere belongs to a distorted dodecahedron with D_{2d} point group and the geometry of Dy2 is seven–coordinate adopts a capped trigonal prism with C_{2v} point group in which the distances are 3.8298(2) Å for Dy1–Dy2, 3.8398(3) Å for Dy2–Dy2a and 10.6356(3) Å for Dy1–Dy1a, respectively. However, it is similar to the reported $[Ln_4(L)_2(HL)_2(NO_3)_2(OH)_2](NO_3)_2$ (Ln = Nd, Yb, Er, Gd) by X.–Q. Lü group.[20] For complex **1**, the salen–type ligand has four chelating modes (Fig. S1) in which the bite angles are in the range of 60.572° to 65.097°, while the bite angles of the reported analogous $[Dy_4(\mu_4\text{-}O)L_2(C_6H_5COO)_6]$[14h] complex are in the range of 63.173° to 66.963°, which are bigger than those of complex **1**.

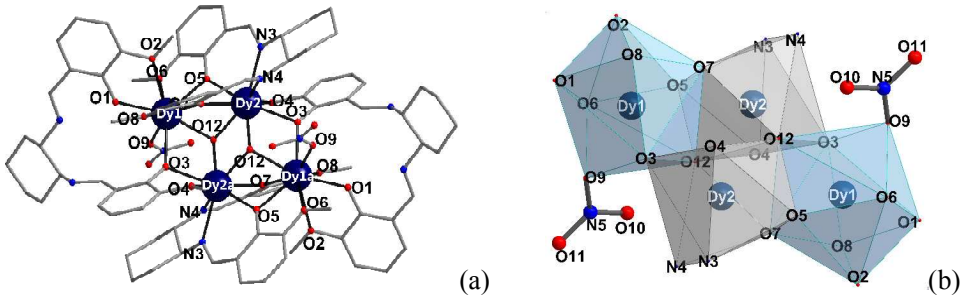

Fig. 1 Molecular structure of the cation for complex **1.** H atoms and solvates are omitted for clarity (a); terminal coordination modes and two coordination geometries of Dy_4 cores (b).

Magnetic Properties

The temperature dependences of the direct current (dc) magnetic susceptibility under an applied dc field of 100 Oe in the temperature range 1.8–300 K (Fig. 2) show that the $\chi_m T$ of complexes **1**–**4** at 300 K are 56.84, 45.37, 55.54 and 42.21 cm^3 K mol^{-1}, respectively, which are close to the expected theoretical values (**1**: 56.68; **2**: 47.28; **3**: 56.28; **4**: 45.92 cm^3 K mol^{-1}) for four non–interacting lanthanide ions. Notably, complexes **1**–**4** present distinct $\chi_m T$–T plots under the same temperature range. With decreasing temperature, the $\chi_m T$ products of complex **1** remains roughly constant from 300 K to 85 K, following by gradually decreased to 57.96 cm^3 K mol^{-1} at 22 K, and then increases sharply to reach a maximum value of 59.6 cm^3 K mol^{-1} at 5 K before decrease suddenly again to a minimum value of 45.05 cm^3 K mol^{-1} at 1.8 K. The decrease of $\chi_m T$ upon lowering temperature in the high–temperature range is most probably governed by the thermal depopulation of the m_J levels of the ground state of the Dy^{III} ion.[23] The increase of $\chi_m T$ at low temperature may be due to the presence of ferromagnetic interaction between the center metal ions. At the lowest temperature, the $\chi_m T$ value decrease sharply again which is likely attributed to zero–field splitting (ZFS), Zeeman effects from the applied field and the competition between ferromagnetic and antiferromagnetic coupling of Dy^{III} ions.[24] The observed phenomenon is in agreement with those reported for similar lanthanide complexes in the literature.[25] In complex **2**, the $\chi_m T$ value undergoes a gradual reduction from 45.37 cm^3 K mol^{-1} at 300 K to 36.07 cm^3 K mol^{-1} at 5 K. Below 5 K, the $\chi_m T$ value drops sharply down to 25.24 cm^3 K mol^{-1} at 1.8 K. It can be attributed to the dominant progressive depopulation of m_J levels split by the crystal–field effect and / or possible antiferromagnetic coupling between Tb^{III} ions.[26] The $\chi_m T$ products of complex **3** slowly decreased from 55.54 cm^3 K mol^{-1} at 300 K to 46.47 cm^3 K mol^{-1} at 16 K, and then sharply increases to 50.54 cm^3 K mol^{-1}at 1.8 K. The decrease of $\chi_m T$ may be due to the depopulation of the m_J levels for a single Ho^{III} ion, and the increase at lowest temperature reveals dominant ferromagnetic interaction between the Ho^{III} center ions in the molecular. For complex **4**, , the $\chi_m T$ value is gradually decreased to the minimums of 18.67 cm^3 K mol^{-1} at 1.8 K upon cooling from 300 K. This continuous decrease may be ascribed to the

depopulation of the m_J levels for a single Er^{III} ion and / or antiferromagntic interactions between Er^{III} ions within tetranuclear units.

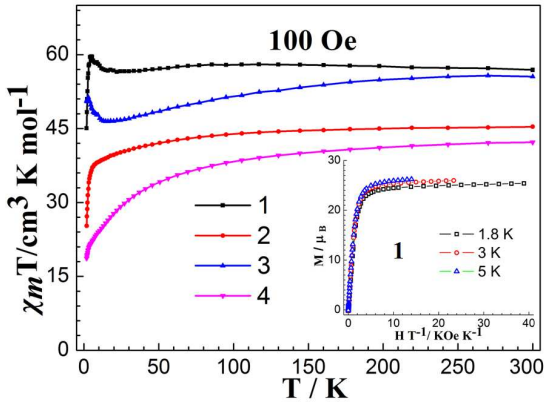

Fig. 2 Temperature dependence of the $\chi_m T$ product at 100 Oe for complexes **1**–**4**. Inset: *M* vs *H/T* plots for complex **1** at different temperatures below 5 K.

The field dependence of the magnetization for complex **1** at 1.8 K, 3 K and 5 K from 0 Oe to 70 KOe shows that the magnetization reaches the maximum of 21.34 μ_B at 1.8 K (Fig. 2, inset). The value of *M* in the low *H* / *T* region becomes more rapidly increased, indicating the ferromagnetic interactions among Dy_4 ions. However, the saturation of 40 $N\mu_B$ is not reached. The non–superposition of the *M vs.H* / *T* data on a single master curve and the high field non–saturation suggests the presence of significant magnetic anisotropy and / or low lying excited states in complex **1**.[19a, 27] The field dependences of the magnetization for complexes **2**–**4** are similar to **1** (Fig. S2). In order to investigate the dynamics of the magnetization which may originate from a single–molecule magnet, ac susceptibility measurements under zero dc field in the temperature range 1.8–25 K at the oscillating frequencies between 1 and 1000 Hz were performed. The obvious frequency dependence is observed in the in–phase (χ') and out–of–phase (χ'') signals for complex **1** (Fig. 3). As the temperature decreases from 20 K to 12 K, the χ'' gradually increase to reach a maximum of 1.37–4.87 cm^3 mol^{-1} from 1000 to 10 Hz and then decrease at even lower temperatures, which indicates that reversal of the spin has been blocked. In addition, with the changing of the ac frequency from 1Hz to 1000 Hz, the

maximum position of the χ'' (T) changes. Obviously, both in–phase (χ') and out–of–phase (χ'') signals for **1** under zero field show slow relaxation of magnetization of SMM behavior. At frequency of 32 Hz and 325 Hz, two peaks are observed which reveal two regimes of relaxation, which may be attributed to the different coordination modes of Dy1 (C_{4v} point group, nine–coordinated with monocapped squared antiprism geometry) and Dy2 (C_{2v} point group, eight–coordinated with distorted dicapped trigonal prism geometry). Although the two slow relaxation processes for complex **1** were observed, it was not so obviously as that reported other salen–type Dy_4[16b, 16c] or Dy_2 SMMs[14d, 16d, 23] with two unequal Dy^{III} ions. In contrast with complex **1**, complex $[Dy_4(salen)_6]\cdot 5.5H_2O$ with two different coordination modes of eight–coordinated of D_{2d} point group and seven–coordinated of C_{2v} point group for four Dy^{III} center ions exhibited two distinct slow relaxation regimes at 1400 Oe dc field. To examine the effect of quantum tunnelling of magnet (QTM), the ac susceptibility measurements were further carried out under an additional dc field of 3600 Oe (Fig. S3). However, only slight shift in the maximum of peaks is observed, which suggests that the additional dc field of 3600 Oe slightly affect the quantum tunnelling of the magnetization.[28] Nevertheless, the two slow magnetic relaxation processes are observed clearly than that under the zero dc field. The temperature–dependent of the ac magnetic susceptibilities (Fig. S4) showed that there is no frequency–dependent signals of the out–of–phase observed at zero dc field but all present frequency–dependent signals and out–of–phase peaks at 3000 Oe dc field for complexes **2**–**4**.

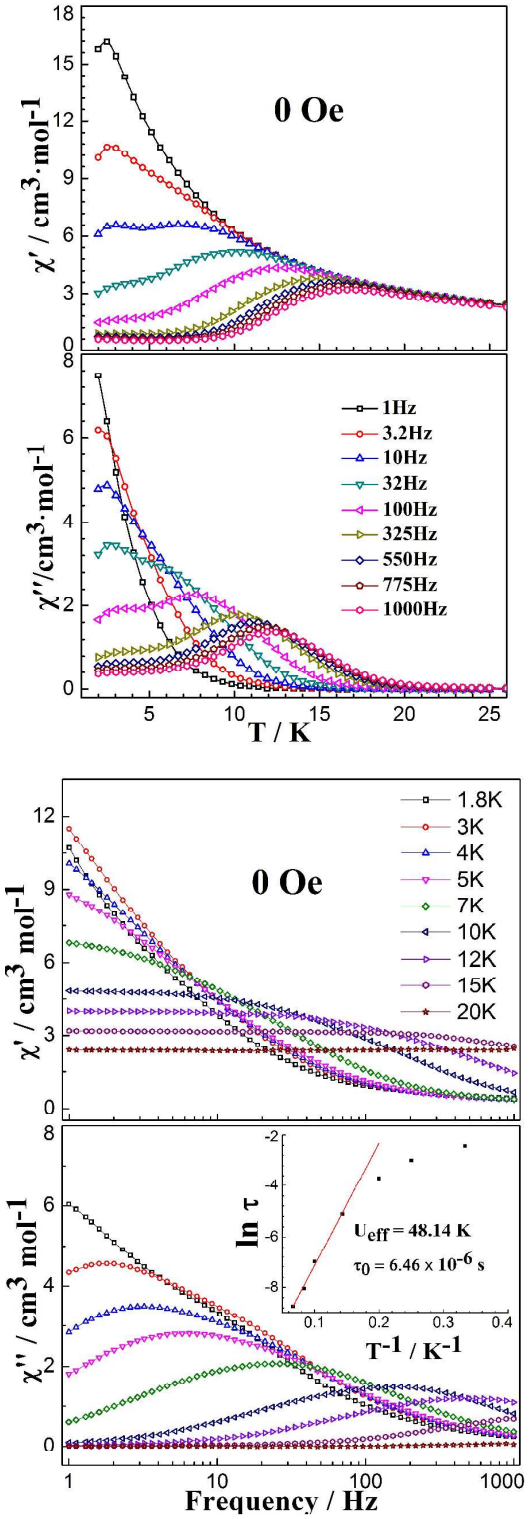

Fig. 3 Temperature dependence of the in–phase (top) and out–of–phase (bottom) ac susceptibility of complex **1** under zero dc field at indicated frequencies.

Fig. 4 Frequency dependence of in–phase (top) and out–of–phase (bottom) ac

susceptibility for **1** under zero dc field; The plots of ln(τ) vs. 1/T for complex **1** under zero dc field, the solid lines represent the fitting with the Arrhenius law (bottom inset).

It is known that the anisotropic energy barrier U_{eff}, can be obtained from the frequency–dependent out–of–phase peak maximum by considering a thermally activated model Arrhenius law, $\tau = \tau_0 \exp(U_{eff}/kT)$. According to the χ'' vs. frequency curve of complex **1** in the high temperature region (Fig. 4 bottom inset), the anisotropic energy barriers is observed at 48.14 K, and the pre–exponential factor of the Arrhenius laws (τ_0) is 6.46×10^{-6} s. To our best knowledge, the effective energy barrier of complex **1** under zero dc field is the largest among the reported pure salen–type tetranuclear lanthanide complexes. E.g. the U_{eff} values of complexes $[Dy_4(salen)_6]\cdot5.5H_2O$[16b], $[Dy_4(\mu_3\text{-}OH)_2L^2{}_2(acac)_6]$[16c] and $[Dy_4(\mu_4\text{-}O)L_2(C_6H_5COO)_6]$[14h] (with bigger bite angles than complex **1**) are 17.2 K, 13.95 K and 2.3 K at zero dc field, respectively. However, it is lower than those reported salen–type Dy_2 complexes, [14a, 14c] especially for those co–coordianted by salen type and halogenated acetylacetone lanthanide complexes. Notably, the anisotropic energy barrier for **1** is attributed to the ligand field of the polydentate bridging ligands and the electron–withdrawing effect of the terminal ligand NO_3^- decreasing the electron density on the Dy^{III} ions.[14a] The plots of χ'' *vs* frequency also confirm the zero–field slow magnetization relaxation of complex **1**, in which the frequency–dependent curves span overlap in a wider range of frequencies at different temperatures without reaching the quantum tunneling of the magnetization regime, which indicate the increase of the energy barrier.

It is known that the simple form of maximizing the effective energy for a particular molecule is to give a highly anisotropic ground state with a large $\pm m_J$ oblate Dy^{III} ion located in sandwich–type ligand geometry.[13,29] However, *N,N'*-bis(3-methoxy-salicylidene)cyclohexane-1,2-diamine is a flexible hexadentate ligand with the outer O_2O_2 moiety, which prefer to form a surrounding crystal field around the lanthanide center ions. The ligand electron density failed to be concentrated above and below the *xy* plane in complex **1**. Thus, the effective energy of complex **1** may be not very high in

contrast with the dysprosium SMMs of sandwich ligand geometry[30] although its effective energy barrier is the highest among the reported salen–type Dy_4 SMMs.

The Cole–Cole plots for **1** under the zero field in the emprature range of 1.8–12 K (Fig. 5) show the symmetric cycles above 7 K and the unsymmetric curves lower than 7 K, which suggest that the two types of relaxation modes exist. Fitting of the Cole–Cole plots by the sums of two modified Debye functions[31] gives relatively large α values in the range of 0.18–0.42. It suggests a relatively wide distribution of relaxation time and the presence of more than one relaxation mode. The change of the circle from unsymmetric to symmetric is similar to that for some polynuclear dysprosium SMMs with different coordination modes under zero dc field.[14d, 23] In order to further confirm the single molecule magnetic properties for complex **1**, the isothermal magnetization experiments have been performed at 1.8 K. However, a very narrow simple sigmoidal hysteresis, the signature of slight anisotropy,[32] was observed. The very small coercivity of the hysteresis loop may be due to the presence of a relatively fast quantum tunneling effect in lanthanide systems (Fig. S5).[33] Such a phenomenon is similar to those reported lanthanide complexes.[34]

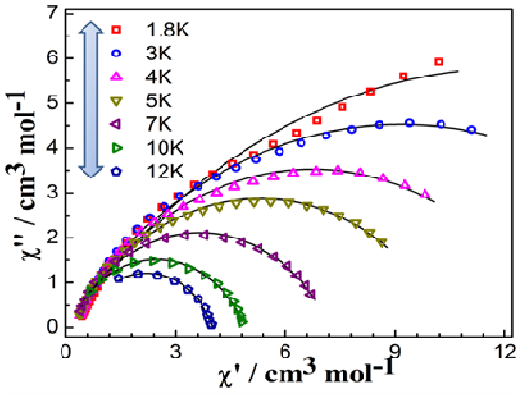

Fig. 5 Cole–Cole plots for **1**obtained using the ac susceptibility data at zero dc field. The solid lines correspond to the best fit obtained with two modified Debye functions.

Conclusions

Isolation of a series of four isomorphic salen type tetranuclear lanthanide complexes verify that *N,N'*-bis(3-methoxy-salicylidene)cyclohexane-1,2-diamine is suitable to coordinate to the lanthanide ions forming discrete tetranuclear structure with a unique $\{Ln_4O_8\}$ core, in which four lanthanide ions are coplanar in a rhombic frame resulting in two crystallographically unequivalent lanthanide ions with C_{4v} point group and C_{2v} point group, respectively. The static and dynamitic magnetic analysis suggests that the nature of the Dy^{III} ions produce the single molecule magnetism for complex **1**. Notably, the ligand of *N,N'*-bis(3-methoxy-salicylidene)cyclohexane-1,2-diamine and the nitrate strengthen the magnetic anisotropy of the Dy^{III} ions resulting in high energy barrier. The two different symmetric lanthanide ions with C_{4v} point group and C_{2v} point group around the lanthanide ions result in two relaxation dynamics for complex **1**.

Acknowledgements

This work is financially supported by the National Natural Science Foundation of China (No. 51272069 & 21471051& 51402092), Heilongjiang Province (No. B 201111).

Notes and references

1. R. Sessoli, D. Gatteschi, A. Caneschi,M. A. Novak, *Nature*, 1993, 141.
2. (a) M. Cavallini, M. Facchini, C. Albonetti, F. Biscarini, *Phys. Chem. Chem. Phys.*, 2008, **10**, 784; (b) J. Gomez-Segura, J. Veciana, D. Ruiz-Molina, *Chem. Comm.*, 2007, 3699; (c) J. D. Rinehart, M. Fang, W. J. Evans, J. R. Long, *Nature Chem.*, 2011, **3**, 538; (d) G. Rogez, B. Donnio, E. Terazzi, J.-L. Gallani, J.-P. Kappler, J.-P. Bucher, M. Drillon, *Adv. Mater.*, 2009, **21**, 4323.
3. (a) B. Donnio, E. Riviere, E. Terazzi, E. Voirin, C. Aronica, G. Chastanet, D. Luneau, G. Rogez, F. Scheurer, L. Joly, J. P. Kappler, J. L. Gallani, *Solid State Sci.*, 2010, **12**, 1307; (b) M. Jenkins, T. Huemmer, M. Jose Martinez-Perez, J. Garcia-Ripoll, D. Zueco, F. Luis, *New J. Phys.*, 2013, **15**; (c) W. Wernsdorfer, N. Aliaga-Alcalde, D. N. Hendrickson, G. Christou, *Nature*, 2002, **416**, 406.
4. (a) L. Jiang, X. Liu, Z. Zhang, R. Wang, *Phys. Lett. A*, 2014, **378**, 426; (b) K. Katoh, H. Isshiki, T. Komeda, M. Yamashita, *Coord. Chem. Rev.*, 2011, **255**, 2124; (c) M. Mannini, F. Pineider, C. Danieli, F. Totti, L. Sorace, P. Sainctavit, M. A. Arrio, E. Otero, L. Joly, J. C. Cezar, A. Cornia, R. Sessoli, *Nature*, 2010, **468**, 417; (d) H. Xie, Q. Wang, H. Jiao, J. Q. Liang, *J. Appl. Phys.*, 2012, **112**; (e) Z. Zhang, L. Jiang, R. Wang, B. Wang, D. Y. Xing, *Appl. Phys. Lett.*,

2011, **99**.

5. D. N. Woodruff, R. E. P. Winpenny, R. A. Layfield, *Chem. Rev.*, 2013, **113**, 5110.
6. (a) M. Atanasov, P. Comba, S. Hausberg, B. Martin, *Coord. Chem. Rev.*, 2009, **253**, 2306; (b) S. Fortier, J. J. Le Roy, C.-H. Chen, V. Vieru, M. Murugesu, L. F. Chibotaru, D. J. Mindiola, K. G. Caulton, *J. Am. Chem. Soc.*, 2013, **135**, 14670; (c) K. E. Vostrikova, *Coord. Chem. Rev.*, 2008, **252**, 1409; (d) Y.-X. Wang, W. Shi, H. Li, Y. Song, L. Fang, Y. Lan, A. K. Powell, W. Wernsdorfer, L. Ungur, L. F. Chibotaru, M. Shen, P. Cheng, *Chem. Sci.*, 2012, **3**, 3366; (e) Y.-Y. Zhu, C. Cui, Y.-Q. Zhang, J.-H. Jia, X. Guo, C. Gao, K. Qian, S.-D. Jiang, B.-W. Wang, Z.-M. Wang, S. Gao, *Chem. Sci.*, 2013, **4**, 1802.
7. N. Ishikawa, M. Sugita, T. Ishikawa, S.-Y. Koshihara, Y. Kaizu, *J. Am. Chem. Soc.*, 2003, **125**, 8694.
8. (a) F. Habib, M. Murugesu, *Chem. Soc. Rev.*, 2013, **42**, 3278; (b) R. Sessoli,A. K. Powell, *Coord. Chem. Rev.*, 2009, **253**, 2328; (c) L. Sorace, C. Benelli, D. Gatteschi, *Chem. Soc. Rev.*, 2011, **40**, 3092; (d) P. Zhang, Y.-N. Guo, J. Tang, *Coord. Chem. Rev.*, 2013, **257**, 1728.
9. (a) P. C. Andrews, G. B. Deacon, R. Frank, B. H. Fraser, P. C. Junk, J. G. MacLellan, M. Massi, B. Moubaraki, K. S. Murray, M. Silberstein, *Eur. J. Inorg. Chem.*, 2009, 744; (b) F. Branzoli, P. Carretta, M. Filibian, G. Zoppellaro, M. J. Graf, J. R. Galan-Mascaros, O. Fuhr, S. Brink, M. Ruben, *J. Am. Chem. Soc.*, 2009, **131**, 4387; (c) B. H. Koo, K. S. Lim, D. W. Ryu, W. R. Lee, E. K. Koh, C. S. Hong, *Chem. Comm.*, 2012, **48**, 2519; (d) P.-H. Lin, W.-B. Sun, Y.-M. Tian, P.-F. Yan, L. Ungur, L. F. Chibotaru, M. Murugesu, *Dalton Trans.*, 2012, **41**, 12349.
10. R. J. Blagg, C. A. Muryn, E. J. L. McInnes, F. Tuna, R. E. P. Winpenny, *Angew. Chem. Int. Ed.*, 2011, **50**, 6530.
11. C. R. Ganivet, B. Ballesteros, G. de la Torre, J. M. Clemente-Juan, E. Coronado, T. Torres, *Chem. -Eur. J.*, 2013, **19**, 1457.
12. (a) D. I. Alexandropoulos, L. Cunha-Silva, P. Linh, V. Bekiari, G. Christou, T. C. Stamatatos, *Inorg. Chem.*, 2014, **53**, 3220; (b) M. U. Anwar, L. N. Dawe, S. S. Tandon, S. D. Bunge, L. K. Thompson, *Dalton Trans.*, 2013, **42**, 7781; (c) H. Zhang, S.-Y. Lin, S. Xue, C. Wang, J. Tang, *Dalton Trans.*, 2014, **43**, 6262; (d) D. N. Woodruff, F. Tuna, M. Bodensteiner, R. E. P. Winpenny, R. A. Layfield, *Organometallics*, 2013, **32**, 1224; (e) S.-Y. Lin, L. Zhao, H. Ke, Y.-N. Guo, J. Tang, Y. Guo, J. Dou, *Dalton Trans.*, 2012, **41**, 3248; (f) N. M. Randell, M. U. Anwar, M. W. Drover, L. N. Dawe, L. K. Thompson, *Inorg. Chem.*, 2013, **52**, 6731.
13. J. D. Rinehart, J. R. Long, *Chem. Sci.*, 2011, **2**, 2078.
14. (a) F. Habib, G. Brunet, V. Vieru, I. Korobkov, L. F. Chibotaru, M. Murugesu, *J. Am. Chem. Soc.*, 2013, **135**, 13242; (b) F. Habib, P.-H. Lin, J. Long, I. Korobkov, W. Wernsdorfer, M. Murugesu, *J. Am. Chem. Soc.*, 2011, **133**, 8830; (c) F. Habib, J. Long, P.-H. Lin, I. Korobkov, L. Ungur, W. Wernsdorfer, L. F. Chibotaru, M. Murugesu, *Chem. Sci.*, 2012, **3**, 2158; (d) P.-H. Lin, W.-B. Sun, M.-F. Yu, G.-M. Li, P.-F. Yan, M. Murugesu, *Chem. Comm.*, 2011, **47**, 10993; (e) J. Long, F. Habib, P.-H. Lin, I. Korobkov, G. Enright, L. Ungur, W. Wernsdorfer, L. F. Chibotaru, M. Murugesu, *J. Am. Chem. Soc.*, 2011, **133**, 5319; (f) H. Wang, C. Liu, T. Liu, S. Zeng, W. Cao, Q. Ma, C. Duan, J. Dou, J. Jiang, *Dalton Trans.*, 2013, **42**, 15355; (g) J. Zhu, H.-F. Song, P.-F. Yan, G.-F. Hou, G.-M. Li, *Crystengcomm*, 2013, **15**, 1747; (h) L. Zhang, P. Zhang, L. Zhao, S.-Y. Lin, S. Xue, J. Tang, Z. Liu, *Eur. J. Inorg. Chem.*, 2013, 1351.
15. F. Yang, P. Yan, Q. Li, P. Chen, G. Li, *Eur. J. Inorg. Chem.*, 2012, 4287.
16. (a) W. Feng, Y. Zhang, Z. Zhang, X. Lu, H. Liu, G. Shi, D. Zou, J. Song, D. Fan, W.-K. Wong,

R. A. Jones, *Inorg. Chem.*, 2012, **51**, 11377; (b) B. H. Koo, K. S. Lim, D. W. Ryu, W. R. Lee, E. K. Koh, C. S. Hong, *Dalton Trans.*, 2013, **42**, 7204; (c) W.-B. Sun, B.-L. Han, P.-H. Lin, H.-F. Li, P. Chen, Y.-M. Tian, M. Murugesu, P.-F. Yan, *Dalton Trans.*, 2013, **42**, 13397; (d) P.-F. Yan, P.-H. Lin, F. Habib, T. Aharen, M. Murugesu, Z.-P. Deng, G.-M. Li, W.-B. Sun, *Inorg. Chem.*, 2011, **50**, 7059.

17. (a) C. Camp, V. Guidal, B. Biswas, J. Pecaut, L. Dubois,M. Mazzanti, *Chem. Sci.*, 2012, **3**, 2433; (b) C. Chen, H. Chen, P. Yan, G. Hou,G. Li, *Inorg. Chim. Acta*, 2013, **405**, 182; (c) B. Gao, Q. Zhang, P. Yan, G. Hou,G. Li, *Crystengcomm*, 2013, **15**, 4167.
18. (a) T. Gao, Y. Yang, W.-B. Sun, G.-M. Li, G.-F. Hou, P.-F. Yan, J.-T. Li, D.-D. Ding, *Crystengcomm*, 2013, **15**, 6213; (b) M. T. Kaczmarek, M. Kubicki, A. Mondry, R. Janicki,W. Radecka-Paryzek, *Eur. J. Inorg. Chem.*, 2010, 2193; (c) S. Liao, X. Yang, R. A. Jones, *Cryst. Growth Des.*, 2012, **12**, 970; (d) X. Yang, M. M. Oye, R. A. Jones, S. Huang, *Chem. Comm.*, 2013, **49**, 9579; (e) X. Zou, P. Yan, J. Zhang, F. Zhang, G. Hou, G. Li, *Dalton Trans.*, 2013, **42**, 13190.
19. (a) C. E. Burrow, T. J. Burchell, P.-H. Lin, F. Habib, W. Wernsdorfer, R. Clerac, M. Murugesu, *Inorg. Chem.*, 2009, **48**, 8051; (b) D. M. Pajerowski, Q. Li, J. Hyun, C. L. Dennis, D. Phelan, P. Yan, P. Chen, G. Li, *Dalton Trans.*, 2014, **43**, 11973; (c) P. Zhang, L. Zhang, S.-Y. Lin, J. Tang, *Inorg. Chem.*, 2013, **52**, 6595.
20. W. Feng, Y. Zhang, X. Lu, Y. Hui, G. Shi, D. Zou, J. Song, D. Fan, W.-K. Wong, R. A. Jones, *Crystengcomm*, 2012, **14**, 3456.
21. CrysAlisPro, *version 171.34.44； Oxford Diffraction Ltd.: Oxfordshire*, 2010, **U.K.**
22. (a) G. M. Sheldrick, *Sheldrick, SHELXL 97, Program for Crystal Structure Refinement, University of Göttingen: Göttingen, Germany* 1997; (b) S. G. M., *Acta Cryst. B*, 2008, **64**, 112.
23. S. Das, A. Dey, S. Biswas, E. Colacio, V. Chandrasekhar, *Inorg. Chem.*, 2014, **53**, 3417.
24. (a) N. Aliaga-Alcalde, R. S. Edwards, S. O. Hill, W. Wernsdorfer, K. Folting, G. Christou, *J. Am. Chem. Soc.*, 2004, **126**, 12503; (b) A. K. Boudalis, B. Donnadieu, V. Nastopoulos, J. M. Clemente-Juan, A. Mari, Y. Sanakis, J.-P. Tuchagues, S. P. Perlepes, *Angew. Chem.Int. Ed.*, 2004, **43**, 2266; (c) C.-F. Wang, W. Liu, Y. Song, X.-H. Zhou, J.-L. Zuo, X.-Z. You, *Eur. J. Inorg. Chem.*, 2008, 717.
25. (a) J.-L. Liu, F.-S. Guo, Z.-S. Meng, Y.-Z. Zheng, J.-D. Leng, M.-L. Tong, L. Ungur, L. F. Chibotaru, K. J. Heroux, D. N. Hendrickson, *Chem. Sci.*, 2011, **2**, 1268; (b) X.-L. Wang, L.-C. Li, D.-Z. Liao, *Inorg. Chem.*, 2010, **49**, 4735; (c) Y.-N. Guo, X.-H. Chen, S. Xue, J. Tang, *Inorg. Chem.*, 2012, **51**, 4035.
26. (a) C. Aronica, G. Pilet, G. Chastanet, W. Wernsdorfer, J.-F. Jacquot, D. Luneau, *Angew. Chem. Int. Ed.*, 2006, **45**, 4659; (b) N. L. Frank, R. Clerac, J. P. Sutter, N. Daro, O. Kahn, C. Coulon, M. T. Green, S. Golhen, L. Ouahab, *J. Am. Chem. Soc.*, 2000, **122**, 2053.
27. (a) H. Ke, L. Zhao, Y. Guo, J. Tang, *Eur. J. Inorg. Chem.*, 2011, 4153; (b) P.-H. Lin, T. J. Burchell, R. Clerac, M. Murugesu, *Angew. Chem. Int. Ed.*, 2008, **47**, 8848; (c) Y. Bi, X.-T. Wang, W. Liao, X. Wang, R. Deng, H. Zhang, S. Gao, *Inorg. Chem.*, 2009, **48**, 11743.
28. G. Abbas, Y. Lan, G. E. Kostakis, W. Wernsdorfer, C. E. Anson, A. K. Powell, *Inorg. Chem.*, 2010, **49**, 8067.
29. P. Zhang, L. Zhang, C. Wang, S. Xue, S.-Y. Lin, J. Tang, *J. Am. Chem. Soc.*, 2014, **136**, 4484.
30. (a) N. Gimenez-Agullo, C. Saenz de Pipaon, L. Adriaenssens, M. Filibian, M. Martinez-Belmonte, E. C. Escudero-Adan, P. Carretta, P. Ballester, J. Ramon Galan-Mascaros,

Chem. -Eur. J., 2014, **20**, 12817; (b) K. Katoh, Y. Horii, N. Yasuda, W. Wernsdorfer, K. Toriumi, B. K. Breedlove, M. Yamashita, *Dalton Trans.*, 2012, **41**, 13582; (c) K. R. Meihaus, J. R. Long, *J. Am. Chem. Soc.*, 2013, **135**, 17952; (d) L. Ungur, J. J. Le Roy, I. Korobkov, M. Murugesu, L. F. Chibotaru, *Angew. Chem. Int. Ed.*, 2014, **53**, 4413.

31. Y.-N. Guo, G.-F. Xu, W. Wernsdorfer, L. Ungur, Y. Guo, J. Tang, H.-J. Zhang, L. F. Chibotaru, A. K. Powell, *J. Am. Chem. Soc.*, 2011, **133**, 11948.
32. A. Borta, E. Jeanneau, Y. Chumakov, D. Luneau, L. Ungur, L. F. Chibotaru, W. Wernsdorfer, *New J. Chem.*, 2011, **35**, 1270.
33. D. Savard, P.-H. Lin, T. J. Burchell, I. Korobkov, W. Wernsdorfer, R. Clerac, M. Murugesu, *Inorg. Chem.*, 2009, **48**, 11748.
34. (a) G. Novitchi, W. Wernsdorfer, L. F. Chibotaru, J.-P. Costes, C. E. Anson, A. K. Powell, *Angew. Chem. Int. Ed.*, 2009, **48**, 1614; (b) Q. Zhou, F. Yang, D. Liu, Y. Peng, G. Li, Z. Shi, S. Feng, *Inorg. Chem.*, 2012, **51**, 7529; (c) F.-Y. Li, L. Xu, G.-G. Gao, L.-H. Fan, B. Bi, *Eur. J. Inorg. Chem.*, 2007, 3405.

Salen–type Dy_4 single–molecule magnet with enhanced energy barrier and its analogues

Fang Luan, [a,b] Pengfei Yan, [a] Jing Zhu, [a] Tianqi Liu, [a] Xiaoyan Zou, [a] Guangming Li*[a]

Graphic abstract

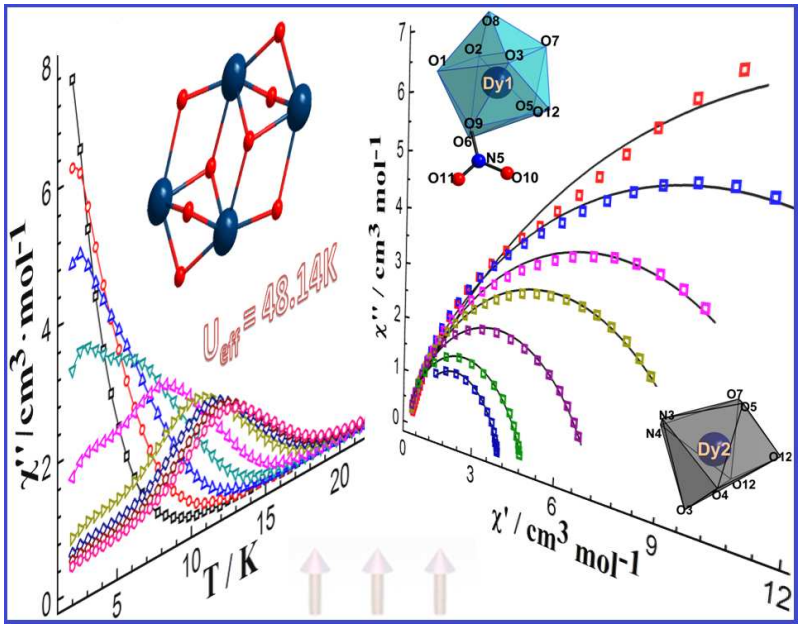

Discrete hexadentate salen–type tetranuclear Dy complex with a unique $\{Ln_4O_8\}$ core exhibits two slow magnetic relaxations with the highest energy barrier of 48.14 K among the reported tetranuclear salen–type dysprosium SMMs.